Mitigation of ionospheric effects on GNSS positioning at low latitudes

Jihye Park

School of Civil and Construction Engineering,

Oregon State University, OR, USA

tel: +1- 541-737-4934, fax: +1- 541-737-3052, e-mail: jihye.park@oregonstate.edu

Sreeja Veettil, Marcio Aquino, Lei Yang

Nottingham Geospatial Institute (NGI),

The University of Nottingham, Nottingham, UK

Claudio Cesaroni

The Istituto Nazionale di Geofisica e Vulcanologia (INGV), Rome, Italy

Abstract

Ionospheric conditions at low latitudes are extremely harsh due to the frequent occurrence of scintillation and the presence of strong TEC gradients. For this study, the São Paulo state region in Brazil is chosen as a test area. This study presents a strategy to mitigate the ionospheric impact on RTK positioning with an experimental result. The proposed strategy explores two approaches that can be applied simultaneously: a) to mitigate the scintillation effect on the GNSS signals by refining the stochastic model of the corresponding observations; and b) to precisely estimate the residual double difference ionospheric delay by exploiting an accurate TEC map.

The strategy was tested on a long baseline kinematic processing under strong scintillation conditions (DOY21 in 2014). Significant improvements were observed when the combined use of the two mitigation approaches described above was compared with the use of conventional state of the art approaches.

1. INTRODUCTION

Appropriate GNSS positioning techniques can currently provide decimeter or even a few centimeters of accuracy. However this is not always true, depending on certain conditions, such as surveying in urban canyons, spoofing or jamming, or a harsh ionospheric environment. These conditions can result in positioning errors several times larger than under normal conditions, making the use of these GNSS techniques unreliable.

CALIBRA (Countering GNSS high Accuracy applications Limitations due to Ionospheric disturbances in BRAzil), a project co-funded by the European GNSS Authority (GSA) under the Seventh Framework Program (FP7), was aimed to mitigate the impact of ionospheric disturbances, such as ionospheric scintillation, on high accuracy GNSS positioning in Brazil. The motivation is that in Brazil there is an increasing demand for highly accurate positioning performance to support applications such as precision agriculture, offshore surveying, land management, civil aviation, geodesy and mapping. Furthermore, due to the geographical location of Brazil across the magnetic equator, high accuracy techniques are particularly affected by ionospheric disturbances. Firstly, ionospheric scintillation frequently occurs during the post sunset hours in Brazil, which can significantly degrade GNSS positioning performance [1]. Secondly, sparse networks of GNSS permanent stations in Brazil present yet another challenge; the long inter-distance between a reference station and a rover affects the positioning performance, especially in the presence of strong ionospheric TEC (Total Electron Content) gradients.

This study provides a strategy to mitigate the effects of the ionospheric disturbances observed in Brazil and shows an experiment where the results compare favorably against conventional

approaches. Section 2 describes the different approaches proposed to mitigate the effects of ionospheric scintillation on GNSS positioning, while section 3 deals with the use of different TEC maps to estimate the background ionospheric corrections. Section 4 describes and discusses the experimental results and the conclusions are shown in section 5.

2. SCINTILLATION MITIGATION BY IMPROVING THE LEAST SQUARES STOCHASTIC MODEL IN GNSS POSITIONING

When the ray path of a satellite passes through irregularity regions of the ionosphere, the signal strength and phase may suffer strong fluctuations, in a phenomenon known as scintillation, which, if severe, affects the positioning performance significantly. One of the strategies to minimize the positioning error due to this effect is to exclude the scintillation-affected satellites. However, eliminating satellites from a positioning solution may weaken the solution geometry, increasing the dilution of precision (DOP) and, consequently, the final positioning accuracy.

Aquino et al. [2] however suggested another approach. They improved the GNSS positioning least squares stochastic model by using the tracking error variance for each satellite/receiver link to weight the corresponding observations. This variance is estimated based on the scintillation indices (i.e. S4 for the amplitude scintillation and σ_ϕ for the phase scintillation) observed by each satellite/receiver link, and is calculated using the receiver tracking models proposed by Conker et al. [3], referred to as the Conker model. The weights are calculated as the inverse of this variance for each satellite/receiver link. According to [3], the model for the L1 C/A code (C1) DLL tracking jitter variance is given by

$$\sigma_{C1}^2 = \frac{B_n d\left[1+{}^{1}\!/_{\eta(c/n0)_{L1-C/A}(1-2S_4^2(L1))}\right]}{2(c/n0)_{L1-C/A}(1-S_4^2(L1))}, \qquad (1)$$

where B_n is the one-sided noise bandwidth, d is the correlator spacing, $(c/n0)_{L1-C/A}$ is the fractional form of signal-to-noise density ratio, η is the pre-detection integration time [2, 3].

The model for the DLL tracking jitter variance for the L2 semicodeless P code (P2) is represented by

$$\sigma_{P2}^2 = \frac{B_n\left[1+{}^{1}\!/_{2\eta(c/n0)_{L1P}(1-S_4^2(L1))}\right]}{2(c/n0)_{L2P}(1-S_4^2(L2))} \qquad (2).$$

The model for the L1 carrier PLL is computed by combining three components, namely a phase scintillation noise ($\sigma_{\phi_s}^2$), a receiver thermal noise ($\sigma_{\phi_T}^2$), and an oscillator noise ($\sigma_{\phi_{osc}}^2$). The closed forms of the phase scintillation and the thermal noise components are provided in (3) and (4), respectively. The oscillator noise is considered as a constant, which varies with the receiver oscillator type.

$$\sigma_{\phi_T}^2 = \frac{B_n\left[1+{}^{1}\!/_{2\eta(c/n0)_{L1-C/A}(1-2S_4^2(L1))}\right]}{(c/n0)_{L1-C/A}(1-S_4^2(L1))} \qquad (3)$$

$$\sigma_{\phi_s}^2 = \frac{\pi T}{k f_n^{p-1}\sin\left(\frac{[2k+1-p]\pi}{2k}\right)} \qquad (4)$$

T is the spectral strength of the phase noise at 1Hz, p is the spectral slope of the phase PSD, k is the order of the PLL, f_n is the loop natural frequency [2]. The details of these tracking jitter models are described in [3].

Although it has been shown that the application of the tracking jitter variances is able to successfully counter scintillation effects [2], there is a limitation as to the level of S4 at which the Conker model can be applied, i.e. the model can only be used if S4 is less than 0.707. From a

thorough investigation aiming to fully understand not only the details of this model but also the various factors affecting the estimation of scintillation effects on GNSS signal tracking, a new amplitude scintillation index was proposed. We called it S4', and it can be applied to the Conker model shown in the equations (1) to (4), leading to a modified approach that we named the Conker' model. The S4' index is generated from the standard deviation of the signal intensity after 1-second-based-normalization. Compared to the original S4, the only difference is the signal to noise ratio normalization procedure, which is carried out at each second, rather than each minute. However, the period for the statistical analysis is the same as for the original S4, i.e. 1 minute. Accordingly, in (1)-(3), c/n0 is updated every second, rather than every minute as in the Conker approach.

As previously mentioned in this section, the variances from the Conker' model contribute to the stochastic model as the inverse of the weights of each observation in the least squares solution. By replacing S4 with S4', the number of epochs when the tracking jitter variance cannot be estimated (due to the limitation of the S4 threshold of 0.707 in the original Conker model) becomes significantly smaller, thus making the system much more robust.

Another approach to compute the tracking jitter variance (and the weights thereafter) in order to improve the least squares stochastic model is what we refer to as the IQ approach, which is based on the signal post correlation In-phase (I) and Quadra-phase (Q) samples. These samples provide information regarding the raw signal properties, and therefore can be used to estimate the tracking jitter variances as in equations (5) and (6) [4].

$$\sigma_{PLL}^2(rad^2) = \left\{std\ \left[\text{atan}\left(\frac{Q}{|I|}\right)\right]\right\}^2 \qquad (5)$$

$$\sigma_{DLL}^2(m^2) = 293.0523^2 \cdot \frac{B_{n_{DLL}}/d}{\left[mean(\sqrt{I^2+Q^2})\right]^2 - \left[2\ std(\sqrt{I^2+Q^2})\right]^2} \quad (6)$$

where $std\left[\text{atan}\left(\frac{Q}{|I|}\right)\right]$ is the standard deviation of the phase tracking error, represented by $\text{atan}\left(\frac{Q}{|I|}\right)$, estimated over the time interval between consecutive observations, 293.0523 is the GPS L1C/A code chip length in meters, $B_{n_{DLL}}$ is the DLL bandwidth and d is an empirically determined parameter related to the correlator spacing and dependent on the signal frequency. For the GPS L1C/A signal, *d* is equal to 10 [4].

In this study these two approaches to improve the least squares stochastic model, respectively by estimating the tracking error variances using the Conker' model or the IQ samples, were tested under the presence of strong scintillation. They were then compared with the conventional weighting methods such as using a constant variance per type of observable, elevation angle based weight, and carrier to noise ratio (*c*/*n*0) based weighting. Additionally, these scintillation mitigation approaches were then used in conjunction with the ionospheric correction methods described in the following section.

3. IONOSPHERIC CORRECTION USING THE CALIBRA TEC MAP (CTM)

The GNSS positioning solution is performed by the Least Squares adjustment computation theory. Eq. (7) shows the Gauss-Markov Model of the Least Squares Solution [5] applied to the GNSS solution,

$$y = A\xi + e,\ \ e \sim (0, \sigma_0^2 W^{-1}) \qquad (7)$$

where y is an observation vector, consisting of dual frequency GNSS double difference observations, ξ is a parameter vector, which contains the corrections to the initial coordinates of the station to be estimated and other unknown parameters such as the ionospheric delay, carrier phase integer ambiguities, etc., A is a design matrix for the double difference observable and corresponding parameters in ξ, e is an observation error vector with the unit variance component σ_0^2 and cofactor matrix W, which constitute together the weight matrix.

For the relative positioning on a short baseline under non-disturbed ionospheric conditions, the double differenced (DD) ionospheric delay is negligible so that the parameters to be estimated are usually three coordinates in the position vector and integer ambiguity parameters of L1 and L2 for DD observations at each single epoch. However if the residual ionospheric delay of each DD observation is not close to zero as in the case of a long baseline, it should be estimated separately, and the number of parameters increases by as many as the number of observed satellites. This case may generate two risks: 1) reduction of redundancy and 2) linear dependency between coefficients of the ionospheric delay and the ambiguity parameter in the design matrix (A) because both parameters are GNSS signal frequency dependent. These risks can be reduced by adding a stochastic constraint [6], as shown in eq. (8).

$$\begin{cases} y = A\xi + e \\ z = K\xi + e_0 \end{cases}; \qquad \begin{bmatrix} e \\ e_0 \end{bmatrix} \sim \left(\begin{bmatrix} 0 \\ 0 \end{bmatrix}, \ \sigma_0^2 \begin{bmatrix} W^{-1} & 0 \\ 0 & Q_0 \end{bmatrix} \right) \tag{8}$$

where z is the a priori information for certain parameters of ξ, K is the corresponding design matrix, e_0 is the error vector of the a priori information, and Q_0 is the corresponding cofactor matrix. External information for the ionospheric delay can be derived from a Total Electron Content (TEC) map for z and the RMS of TEC for e_0. Unlike fixed constraints, the stochastic

constraints in (8) allow the system better flexibility by providing the variances of the prior information in Q_0 [6].

There are several global and local ionospheric maps, which can be used to introduce external ionospheric information in GNSS positioning. One of the most accessible products is the Global Ionosphere Map (GIM) provided by the International GNSS Service (IGS). Currently, vertical TEC (vTEC) maps are generated independently by four centers, i.e. CODE (Center for Orbit Determination in Europe), ESA (European Space Agency), JPL (Jet Propulsion Laboratory) and UPC (Polytechnic University of Catalonia). The IGS combines them to generate the combined TEC map as a final product [14].

On the other hand, a local TEC map over the São Paulo state was created under the CALIBRA project [15], referred to as the CALIBRA TEC map (CTM).

The CTM is generated by using GNSS data from a regional network of 50 Hz GNSS receivers deployed in the framework of the FP7/GSA projects CIGALA and CALIBRA, covering the São Paulo state region. The GNSS stations used to generate the CTM are indicated as blue triangles in Figure 1. These vTEC maps, constructed using a finer grid than the one used by the IGS in the GIM, rely on a calibration technique that is able to provide slant TEC (sTEC) values free from biases due to multipath and errors affecting the GNSS observables. The technique, developed by Ciraolo et al. [9] makes use of both code and phase observables, in the so-called 'carrier to code levelling process', which is performed for each continuous arc of observation. The dual frequency carrier phase and code GNSS measurements can be used in the geometry-free linear combination to estimate the ionospheric delay, as represented respectively by eq. (9) for the phase and eq. (10) for the code:

$$\tilde{L}_{arc} = sTEC + B_R + B_S + C_{arc} + \varepsilon_L \quad (9)$$

$$P = sTEC + b_R + b_S + \varepsilon_P \quad (10)$$

Where B_R, B_S are the carrier phase receiver and satellite inter frequency biases (IFBs) and b_R, b_S are the equivalent code IFBs, C_{arc} is the phase ambiguity and ε_L, ε_P are the noise on the carrier-phase and code respectively. To carry out the levelling procedure, the mean, over a continuous arc of observation, of the difference of the code and the carrier-phase measurements is subtracted from the carrier-phase (see Ciraolo et al, 2007 [9] for more details), leading to:

$$\breve{L}_{arc} = sTEC + b_R + b_S + \langle \varepsilon_P \rangle_{arc} + \varepsilon_L \quad (11)$$

Where $\breve{L}_{arc}$ is the carrier-phase ionospheric delay observable 'levelled' to the code ionospheric observable. This procedure is known as the 'carrier to code levelling process'.

As demonstrated by [10], ε_L can be neglected and usually also $\langle \varepsilon_P \rangle_{arc}$, representing the average over an arc of observation of the noise on the carrier-phase, is assumed to be equal to zero. In the approach used in this work $\langle \varepsilon_P \rangle_{arc}$ is not neglected and the bias affecting $\breve{L}_{arc}$ is estimated considering $b_R + b_S + \langle \varepsilon_P \rangle_{arc}$ as a single error affecting the measurement, as represented in equation (12):

$$\tilde{L}_{arc} = sTEC + \beta_{arc} \quad (12)$$

Where $\tilde{L}_{arc}$ phase levelled measurements and β_{arc} represents the contribution of all the biases affecting a continuous arc of observation. The sTEC values obtained in this process are projected to vertical using the well-known thin shell approximation and the cos χ mapping function [11]. At low latitudes the thin shell assumption can lead to non-negligible errors in the estimation of the vTEC values, but if the GNSS network can ensure a good coverage of the area of interest as in the case of this study,

this simple assumption can be used as demonstrated in [16]. Taking advantage from the accurate TEC values obtained using the calibration technique and from the good data coverage ensured by the CIGALA/CALIBRA network, the CTM is used to properly describe the peculiar conditions of the Brazilian ionosphere.

The performances of the GIM and the CTM were evaluated in terms of the positioning errors obtained in the long baseline kinematic positioning described in the next section.

4. EXPERIMENTAL RESULTS

As mentioned in the previous section, the CTM was generated using high rate GNSS data from selected stations in the São Paulo state region, shown in Figure 1 as blue triangles. The other high rate GNSS stations shown in Figure 1 as red triangles, although part of the network, did not contribute to the CTM generation. All stations in the network are equipped with PolaRxS receivers which are capable of recording 50Hz high rate data (which contain the I and Q components), as well as the phase (σ_ϕ) and amplitude (S4) scintillation indices. In order to verify the potential improvement by applying the newly developed scintillation mitigation techniques and the CTM, we selected a long baseline (88.4km) made up of stations SJCU (fixed) and EEAR (rover), for kinematic post processing. Results were evaluated based on the estimated coordinates of station EEAR, which did not contribute to the CTM generation. For the tracking jitter variance estimation we used the constant based (i.e. constant variance per observable type), elevation based, c/n0 based, Conker' based and IQ based approaches. The first 3 are classed as conventional state of the art non-mitigated (i.e. non-scintillation sensitive) approaches and the last 2 as newly developed scintillation mitigated approaches. It should be noted that the experiments in this study were conducted using an in-house RTK software which allowed implementations of the variances estimated from S4' or IQ as well as the external information

from the TEC maps. Ambiguity resolution was performed using the LAMBDA method [7] and validated using the W-ratio test [8]. The tropospheric delay was calculated using the Saastamoinen model [12] with the Global mapping function [13].

Figure 1: Scintillation monitoring GNSS stations in the São Paulo state region

Figure 2 indicates the S4 recorded at SJCU station on the selected day, DOY21 in 2014. From 0-6 UT hours and 22-24 UT hours, the S4 indices reached greater than 1, which is considered as an extremely strong scintillation.

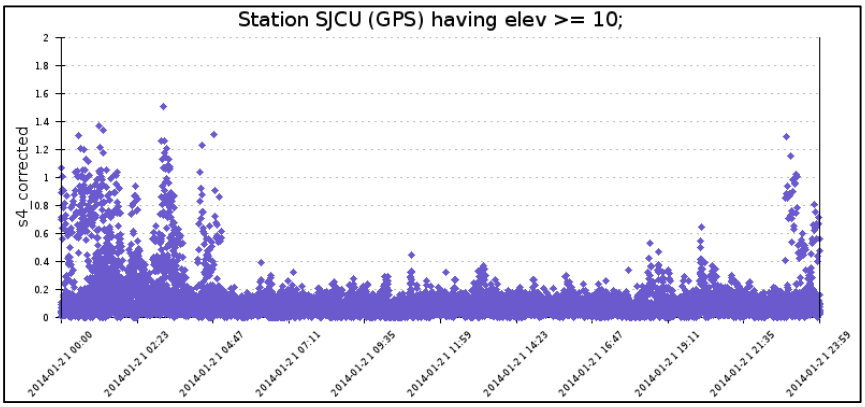

Figure 2: S4 recorded at SJCU on DOY21 in 2014 (time is in UT)

Figure 3 shows the time series plots of selected positioning results. The upper plot shows one of the conventional methods which applies the c/n0 based weighting combined with the GIM and the bottom plots are the proposed strategies for scintillation mitigation methods, Conker' and IQ, both combined with the CTM. The firs three plots from the top in each panel show the

positioning error in north, east, and up components respectively and the bottom plot indicates the ambiguity resolution result (1: fixed solution, 0: float solution).

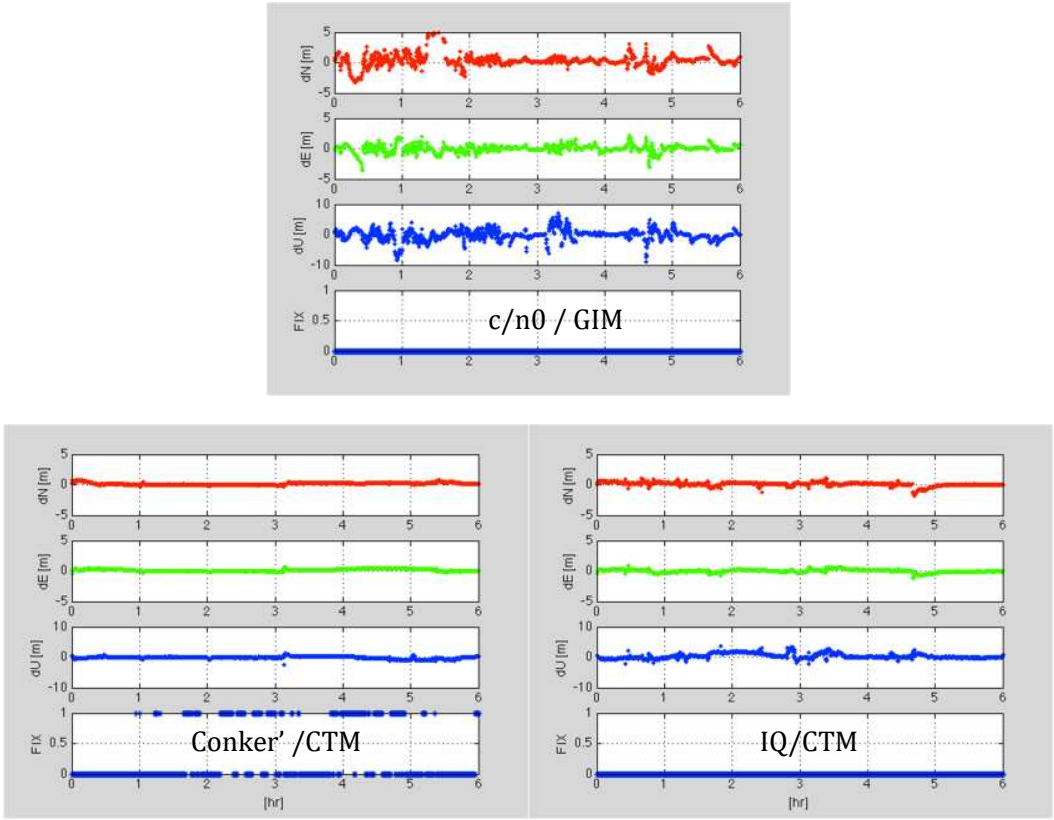

Figure 3: GNSS kinematic positioning results on DOY21, 2014 (0-6 UT hours) with the non-mitigated approach (c/n0) with the GIM (upper), Conker' approach with the CTM (lower left), and IQ approach with the CTM (lower right). Top three plots in each panel represent the positioning error in north, east, and up components and the bottom plot indicates the ambiguity fixed (1) or float (0) solutions of corresponding epochs.

From the figure, it can be clearly seen that the Conker' and CTM approach located in the low left corner includes less noise in positioning result and more fixed solution than the other two approaches. Table 1 summarizes the GNSS positioning results with the different weighting methods using different TEC maps during the strong scintillation hours on DOY21 in 2014. The first column indicates the weighting method and the TEC map applied in each test. The following columns show the success rate of the ambiguity resolution (AR) with

the positioning RMS for the ambiguity fixed solutions, positioning errors of the float solutions, and overall RMS, all in meters. For the fixed solutions, some were incorrectly fixed, increasing their overall RMS. Therefore, we additionally analyzed the epochs with RMS ≤ 10cm, which we considered to be the correctly fixed solutions, which are all quite low level of success rate. Consequently, we focused on the RMS of all solution for the performance evaluation of suggested approaches.

It should be emphasized that in absolute terms the positioning performances of all these tests are very poor due to the extremely strong scintillation conditions. However the purpose of this study is to demonstrate the advantage of applying the proposed strategies over the use of the existing conventional approaches. It can be clearly seen that the scintillation mitigation techniques always yield the best and the second best positioning results when applied with either of the maps. Moreover, the CTM performs better than the GIM with most weighting methods as highlighted in Table 1.

Table 1: Positioning result for combined algorithm of scintillation mitigation and TEC correction on long baseline during the strong scintillation hours (0-6 UT hr) on DOY21 in 2014

2014/021	**DOY021 in 2014 (15sec) SJCU-EEAR, 88.4km baseline**					
	Fixed				**Float**	**All**
	AR [%]	**RMS [m]**	**≤10cm AR [%]**	**≤10cm RMS [m]**	**RMS [m]**	**RMS [m]**
Const[1]-GIM	3.2%	0.101m	1.4%	0.092m	1.173m	1.139m
Elev[2]-GIM	4.3%	0.058m	4.3%	0.058m	1.893m	1.814m
CN0[3]-GIM	0%	NA	0%	NA	1.794m	1.794m

Conker'[4]-GIM	12.8%	1.090m	8.5%	0.057m	1.446m	1.400m
IQ[5]-GIM	0%	NA	0%	NA	0.880m	0.880m
Const-CTM	0%	NA	0%	NA	1.654m	1.654m
Elev-CTM	0%	NA	0%	NA	1.159m	1.159m
CN0-CTM	4.2%	1.254m	0%	NA	1.809m	1.786m
Conker'-CTM	29.0%	0.360m	5.0%	0.061m	0.433m	0.412m
IQ-CTM	0%	NA	0%	NA	0.756m	0.756m

1: weighting based on Constant variance per observable; 2: weighting based on elevation angle; 3: weighting based on carrier to noise ratio; 4: weighting based on Conker' model; 5: weighting based on IQ samples.

In the case study presented in this paper, the 3D positioning RMS error obtained by applying the elevation based approach, together with the GIM reached up to 1.814m during the post sunset strong scintillation hours (0:00-6:00 UT), whereas when applying the Conker' based technique in conjunction with the CTM, the result was significantly improved, with a 3D positioning RMS of 0.412 m. The greatest improvement, of 77.3%, is obtained by using Conker' combined with the CTM. The IQ based technique with the CTM, which is the second best combination, achieved an improvement of 58.3% with a 3D RMS of 0.756m. The best result among the conventional approaches was the use of the GIM combined with the constant variances per observable, with a 3D RMS of 1.139m. This is still less than the improvements of 63.8% and 33.6%, respectively obtained by using the Conker' with the CTM and the IQ with the CTM. In addition, it can be observed that the IQ showed the best performance when only the GIM is available.

5. CONCLUSIONS

Under severe ionospheric scintillation conditions, the GNSS kinematic positioning performance is generally very poor. In order to tackle the scintillation effects which are prevalent at low latitudes, this paper presents two strategies to improve the least squares stochastic model, based respectively on the use of the newly proposed Conker' model and the IQ samples to estimate tracking error variances. To deal with the background residual ionospheric effects, the use of a local TEC map, the CTM, is compared with the use of a Global Ionospheric Map (GIM).

From this case study, 3 main conclusions can be drawn: 1) both of the proposed scintillation mitigation approaches successfully reduce the positioning error in comparison to the conventional, non-mitigated approaches; 2) the CTM performs consistently better than the GIM under any of the circumstances during the experiment and 3) by combining these two techniques developed during the CALIBRA project, i.e. scintillation mitigation algorithms and the ionospheric correction using the CTM, the positioning performance can be significantly improved.

The proposed strategy shows that an advanced stochastic model and proper TEC information can greatly improve the GNSS positioning performance under disturbed ionospheric conditions.

ACKNOWLEDGMENTS

The CALIBRA project was funded under the European Commission 7th Framework Program and is carried out in the context of the Galileo FP7 R&D program supervised by the European GNSS Agency (GSA). The authors would like to thank all CALIBRA partners, including UNESP (São Paulo State University, Brazil), Septentrio Satellite Navigation NV, INGV (Istituto Nazionale di Geofisica e Vulcanologia, Italy) and UNG (University of Nova Gorica, Slovenia) for their collaboration, and the GSA for the financial support.

REFERENCES

1. Sreeja V., Aquino, M., Elmas, Z. G., Forte, B., "Correlation analysis between ionospheric scintillation levels and receiver tracking performance", *Space Weather*, 10(6): S06005, 2012, doi:10.1029/2012SW000769.

2. Aquino, M., Monico, J. F. G., Dodson, A. H., Marques, H., Franceschi, G., Alfonsi, L., Romano, V., and Andreotti, M., "Improving the GNSS positioning stochastic model in the presence of ionospheric scintillation", *Journal of Geodesy*, 83(10), 2009, pp. 953–966, doi:10.1007/s00190-009-0313-6.

3. Conker, R. S., El-Arini M. B., Hegarty, C. J., Hsiao, T., "Modeling the effects of ionospheric scintillation on GPS/satellite-based augmentation system availability", *Radio Science*, 38(1):1001, 2003, doi:10.1029/ 2000RS002604.

4. Elmas, Z. G., "Exploiting New GNSS signals to monitor, model and mitigate the ionospheric effects in GNSS", *PhD dissertation*, Nottingham Geospatial Institute, The University of Nottingham, Nottingham, UK, 2013.

5. Groß, J., "The general Gauss-Markov model with possibly singular dispersion matrix", Statist. Pap. 45:311–336, 2004.

6. Schaffrin B. and Navratil G., "On Reproducing Linear Estimators within the Gauss–Markov Model with Stochastic Constraints", *Communications in Statistics – Theory and Methods*, 41(13-14): 2570-2587, 2012, DOI:10.1080/03610926.2011.631073.

7. Teunissen P. J. G., A new method for fast carrier phase ambiguity estimation, *Proceedings IEEE PLANS*, Las Vegas, NV, 11-15, April, 1994, pp. 562-573.

8. Wang J., Stewart M., and Tsakiri M., "A discrimination test procedure for ambiguity resolution on-the-fly", Journal of Geodesy, 72: 644-653, 1998.

9. Ciraolo, L., Azpilicueta, F., Brunini, C., Meza, a. and Radicella, S. M.: Calibration errors on experimental slant total electron content (TEC) determined with GPS, J. Geod., 81, 111–120, doi:10.1007/s00190-006-0093-1, 2007.

10. Braasch, M.S. Global Positioning System: Theory and Applications. Chapter 14: Multipath Effects, vol. 1, American Institute of Aeronautics and Astronautics, Reston, VA, USA, 547–568, 1996, DOI: 10.2514/5.9781600866388.0547.0568.

11. Mannucci, a. J., Wilson, B. D., Yuan, D. N., Ho, C. H., Lindqwister, U. J. and Runge, T. F.: A global mapping technique for GPS-derived ionospheric total electron content measurements, Radio Sci., 33(3), 565, doi:10.1029/97RS02707, 1998.

12. Saastamoinen J., "Contributions to the theory of atmospheric refraction", Bulletin Geodesique, 105(1): 279–298, 1972.

13. Boehm J., Niell A. E., Tregoning P., and Schuh H., "Global Mapping Functions (GMF): A new empirical mapping function based on numerical weather model data", Geophysical Research Letters, 33: L07304, 2006, doi:10.1029/2005GL025545.

14. Hernández-Pajares M., Juan J. M., Sanz J., Orus R., Garcia-Rigo A., Feltens J., Komjathy A., Schaer S. C., and Krankowski A., "The IGS VTEC maps: a reliable source of ionospheric information since", Journal of Geodesy, 83(3-4), 1998, pp. 263-275.

15. Cesaroni C., “A multi instrumental approach to the study of equatorial ionosphere over South-America”, PhD dissertation, University Alma Mater studiorum, Bologna, Italy. 2015, doi: 10.6092/unibo/amsdottorato/6889.

16. Cesaroni C, Spogli L, Alfonsi L, De Franceschi G, Ciraolo L, et al. L-band scintillations and calibrated total electron content gradients over Brazil during the last solar maximum. J. Space Weather Space Clim., 5, A36, 2015, DOI: 10.1051/swsc/2015038